Developmentally programmed remodeling of the *Drosophila* olfactory circuit

Elizabeth C. Marin[1], Ryan J. Watts[1], Nobuaki K. Tanaka[2], Kei Ito[2] and Liqun Luo[1,*]

[1]Department of Biological Sciences, Stanford University, Stanford, CA 94305, USA
[2]Institute of Molecular and Cellular Biosciences, The University of Tokyo, Tokyo 113-0032, Japan
*Author for correspondence (e-mail: lluo@stanford.edu)

Accepted 9 December 2004

Development 132, 725-737
Published by The Company of Biologists 2005
doi:10.1242/dev.01614

Summary

Neural circuits are often remodeled after initial connections are established. The mechanisms by which remodeling occurs, in particular whether and how synaptically connected neurons coordinate their reorganization, are poorly understood. In *Drosophila*, olfactory projection neurons (PNs) receive input by synapsing with olfactory receptor neurons in the antennal lobe and relay information to the mushroom body (MB) calyx and lateral horn. Here we show that embryonic-born PNs participate in both the larval and adult olfactory circuits. In the larva, these neurons generally innervate a single glomerulus in the antennal lobe and one or two glomerulus-like substructures in the MB calyx. They persist in the adult olfactory circuit and are prespecified by birth order to innervate a subset of glomeruli distinct from larval-born PNs. Developmental studies indicate that these neurons undergo stereotyped pruning of their dendrites and axon terminal branches locally during early metamorphosis. Electron microscopy analysis reveals that these PNs synapse with MB γ neurons in the larval calyx and that these synaptic profiles are engulfed by glia during early metamorphosis. As with MB γ neurons, PN pruning requires cell-autonomous reception of the nuclear hormone ecdysone. Thus, these synaptic partners are independently programmed to prune their dendrites and axons.

Key words: Olfaction, Projection neuron, Metamorphosis, Pruning, Steroid hormone, TGFβ signaling, Antennal lobe, Mushroom body, Lateral horn, *Drosophila*

Introduction

Structural and functional changes in neuronal connectivity extending past embryogenesis and even into adult life are of great interest to neurobiologists. One of the most dramatic examples of reorganization of neuronal connectivity is that which occurs during metamorphosis in holometabolous insects, which possess two distinct nervous systems at the larval and adult stages. Many neurons are born during larval and pupal stages to function specifically in the larger, more complex adult nervous system. Other neurons are used only in the simpler larval nervous system and die during metamorphosis. But a third class of neurons are morphologically differentiated and likely to function in both the larval and the adult systems; they do so by reorganizing their dendrites and axons during metamorphosis (reviewed by Tissot and Stocker, 2000; Truman, 1990).

One of the best-studied examples of neuronal reorganization in an insect central nervous system is the γ neuron of *Drosophila* mushroom bodies (MBs) (Technau and Heisenberg, 1982; Armstrong et al., 1998; Lee et al., 1999; Lee et al., 2000; Watts et al., 2003; Watts et al., 2004; Zheng et al., 2003; Awasaki and Ito, 2004). MB γ neurons are born during embryonic (Armstrong et al., 1998) and early larval stages (Lee et al., 1999). They send dendrites into the MB calyx and axons into larval medial and dorsal MB axon lobes. During early metamorphosis, γ neurons prune their larva-specific dendrites and axon branches before re-extending adult-specific processes (Lee et al., 1999). What happens to their synaptic partners while MB γ neurons reorganize their dendrites and axons? In this study, we show that a subset of olfactory projection neurons – the major presynaptic partners of MB γ neurons – are also morphologically differentiated to function in both larva and adult. We also show that the reorganization of these neurons during metamorphosis is independently controlled by some of the same molecular mechanisms as that of the MB γ neurons.

In the adult fly, odors are detected by olfactory receptors (ORs) on the dendrites of about 1300 olfactory receptor neurons (ORNs) in the antennae and maxillary palps. In general, each ORN appears to express one of ~45 possible OR types (Clyne et al., 1999; Gao and Chess, 1999; Vosshall et al., 1999), and the axons of all ORNs expressing a given OR converge to one of ~45 stereotypical glomeruli in the antennal lobe (AL), the equivalent of the mammalian olfactory bulb (Gao et al., 2000; Vosshall et al., 2000). From there, 150-200 projection neurons (PNs) relay olfactory activity to higher brain centers, the MB calyx and the lateral horn (LH) of the protocerebrum (Stocker, 1994). Systematic clonal analysis using the MARCM method (Lee and Luo, 1999) to label single and clonally related clusters of PNs that express the GAL4

driver GH146 (Stocker et al., 1997) revealed that these PNs are prespecified by lineage and birth order to innervate particular glomeruli in the adult AL (Jefferis et al., 2001). Moreover, each glomerular class of PNs exhibits a characteristic axon branching pattern in the LH, suggesting stereotyped targets in at least one higher olfactory center (Marin et al., 2002; Wong et al., 2002).

The *Drosophila* larval olfactory system is much smaller and simpler by comparison (Cobb and Domain, 2000; Heimbeck et al., 1999), shown to consist of only 21 ORNs in the dorsal organ (Singh and Singh, 1984) and believed to include ~50 PNs relaying information to the larval MB and LH (Python and Stocker, 2002; Stocker, 1994). Developmental analysis has shown that the PNs born during larval stages exhibit only a single unbranched process from the cell body to the MB calyx until early metamorphosis, when dendrites and axon terminal branches start to elaborate (Jefferis et al., 2004). Thus, larval-born PNs do not participate in the larval olfactory circuit.

What, then, is the origin of the relay interneurons that connect the larval AL to higher olfactory centers? Do they contribute to the adult olfactory system as well? Here we show that, in contrast to the larval-born PNs, PNs generated during embryogenesis exhibit morphologically differentiated dendrites and axons in both larva and adult. These neurons prune their processes locally during the first few hours of metamorphosis and later re-extend them to innervate developing adult structures. This pruning process is regulated by ecdysone and TGFβ signaling, as has been demonstrated previously for MB γ neurons (Lee et al., 2000; Zheng et al., 2003). Thus, developmentally programmed remodeling allows these embryonic-born PNs to participate in two distinct olfactory circuits at two different stages in the *Drosophila* life cycle.

Materials and methods

Fly strains and staging

To label wild-type PNs using MARCM, embryos of genotype y w hs-FLP UAS-mCD8-GFP/(w or Y); FRT^{G13} tubP-GAL80/FRT^{G13} GAL4-GH146 UAS-mCD8-GFP or y w hs-FLP^{122} UAS-mCD8-GFP/(y w or Y); FRT^{G13} tubP-GAL80/FRT^{G13} GAL4-GH146 UAS-mCD8-GFP were heat-shocked at 37°C for 1 hour to induce mitotic recombination. The following mutant stocks were used to perform MARCM: y w hs-FLP UAS-mCD8-GFP/(w or Y); FRT^{G13} tubP-GAL80/FRT^{G13} *babo*^{Fd4} GAL4-GH146 UAS-mCD8-GFP or y w hs-FLP^{122}/(y w or Y); FRT^{G13} tubP-GAL80/FRT^{G13} *babo*^{Fd4} GAL4-GH146 UAS-mCD8-GFP and y w hs-FLP^{122} FRT^{19A} tubP-GAL80/FRT^{19A} *usp*^{3}; GAL4-GH146 UAS-mCD8-GFP. hs-FLP^{122} is a more active FLP insertion line used to generate MARCM clones at higher frequency (kind gift of M. Metzstein and M. Krasnow, Stanford University). In addition, y w; GAL4-MZ612 UAS-mCD8-GFP and y w; GAL4-GH146 UAS-mCD8-GFP homozygous flies were dissected to examine holo-GAL4 expression.

All embryos were collected on grape juice agar plates at 25°C. For embryonic heatshock, embryos were stored at 16°C before and until 24 hours after the heatshock; the temperature was then raised stepwise through 18°C, 20°C, and finally 25°C to prevent unintentional hs-FLP induction. Wandering third instar larvae were collected and dissected immediately. White pre-pupae were collected and then aged at 25°C for the desired number of hours prior to dissection.

Dissection and immunohistochemistry

Adult brain dissection and immunostaining were according to protocols described previously (Jefferis et al., 2001). Larval and pupal brains were dissected and stained using a protocol modified from Python and Stocker (Python and Stocker, 2002). Briefly, brains were dissected into phosphate-buffered saline (PBS) with 0.2% Triton-X and fixed in 4% paraformaldehyde for 1-2 hours at 4°C. Brains were then washed three times in PBS-Triton and blocked in 3% normal goat serum at room temperature, and incubated overnight at 4°C with rat monoclonal anti-mCD8 α subunit (Caltag, Burlingame, California) at 1:100 and either mouse monoclonal nc82 (kind gift of E. Buchner, University of Wuerzberg) at 1:20, rabbit polyclonal anti-synaptotagmin (kind gift of H. Bellen, Baylor College of Medicine) at 1:1000, or mouse monoclonal anti-EcRB1 (AD4.4, kind gift of C. Thummel, University of Utah) at 1:5000. Brains were again washed three times in PBS-Triton at RT and incubated overnight at 4°C with Alexa-488 goat anti-rat IgG at 1:300 and Alexa-568 goat anti-mouse IgG or Alexa-568 goat anti-rabbit IgG at 1:300 (Molecular Probes, Eugene, OR). Brains were washed, equilibrated using the Slow-Fade Light Anti-Fade Kit (Molecular Probes, Eugene, OR), and whole mounted on glass slides.

Confocal and electron microscopy

Stacks of optical confocal sections at 1-2 μm spacing were obtained with a Bio-Rad MRC 1024 laser-scanning confocal microscope using the Laser Sharp image collection program. Raw images were processed using the freeware program ImageJ and the commercial software Adobe Photoshop. Presented images are either single slices or flattened confocal stacks, as indicated. Electron microscopy studies were performed as previously described (Watts et al., 2004).

Clonal analysis

We observed single-cell clones innervating adult AL glomeruli VL2p+, DP1m, DP1m+DM4, VA2, VA6, VL2a, VL2a+DC1, DC1, VA7l, DA4, DM3, DM7, VM3, DL6 and either D or a glomerulus just posterior. In addition, we saw DL2d and DP1m-independent DM4 labeling in Nb clones, although not as yet in any single-cell clones. From this available set, we selected eight landmark glomeruli (DP1m, VL2p, VA6, VA2, DL5, DM3, VM3 and DL6) for the neuroblast clone birth order study.

In the analysis of mutants (*usp* or *babo*), it is in theory possible that some of the MARCM phenotypes were caused by non-autonomous effects of neurons that were homozygous mutant but not labeled by GAL4-GH146. We think this is unlikely because the frequency of mitotic recombination induced by heatshocking during embryogenesis is extremely low (1-2 orders of magnitude lower than heatshocking in larvae). Given the penetrance of the phenotypes, it is unlikely that coincident unlabeled homozygous clones could account for the defects observed.

Results

Embryonic-born projection neurons participate in the adult olfactory system

The MARCM method allows the labeling of a single neuron, or all neurons born from the same neuroblast, that express a particular GAL4 driver. We focused our studies on the ~90 (out of an estimated total 150-200) PNs that express GAL4-GH146 (Stocker et al., 1997; Jefferis et al., 2001). We used a heatshock-promoter-driven FLP recombinase to control the timing of the mitotic recombination that results in labeled MARCM clones (see Materials and methods). In a previous study (Jefferis et al., 2001), we identified at least one GAL4-GH146-positive PN that could only be labeled by heatshock-induced mitotic recombination during embryogenesis. This embryonic-born PN specifically targeted its dendrites to glomerulus VA2, one of many glomeruli innervated when

labeling the entire population of GH146 PNs (Fig. 1A), yet never by PN single-cell or neuroblast clones labeled by heatshock during larval stages (Fig. 1B,C). This discrepancy in the number of innervated glomeruli suggested that a fraction of adult AL glomeruli were being targeted by a subset of PNs born during embryogenesis.

To study the embryonic-born neurons labeled by the GH146 driver, we systematically generated MARCM clones by heatshock induction at embryonic stages. We found that large anterodorsal neuroblast clones labeled by heatshock early in embryogenesis innervated at least 15 glomeruli not targeted by either the anterodorsal or lateral neuroblast clones labeled by heatshocking newly hatched larvae (Fig. 1D; see Materials and methods for details). We used MARCM single-cell clones to characterize embryonic-born PNs that innervate eight different landmark glomeruli in the adult AL (Fig. 1E1-L1). The gross morphology of these PNs in the adult brain is quite similar to that of the larval-born PNs previously described (Jefferis et al., 2001; Marin et al., 2002): each PN generally innervates a single glomerulus in the antennal lobe (distinct from those innervated by larval-born PNs), then sends its axon via the inner antennocerebral tract to display a characteristic terminal branching pattern in the LH according to its glomerular class, along with a number of collaterals in the MB calyx that end in prominent boutons (Fig. 1E2,E3-L2,L3). Detailed analysis of the stereotypy of these axons using quantitative methods will be reported elsewhere (G. Jefferis, C. Potter, A. Chan, E.C.M., T. Tohlfing, C. Maurer and L.L., unpublished).

By comparing the specific glomeruli innervated in each partial anterodorsal neuroblast clone generated by heatshock at different times during embryogenesis (n=73), we ascertained that: (1) these embryonic-born PNs were generated in the order DP1m, VL2p, VA6, VA2, DL5, DM3, VM3 and finally DL6 (Table 1); and (2) every clone labeled by embryonic heatshock included all of the larval-born anterodorsal PNs analyzed in our previous study, indicating that both PN subsets originate from the same neuroblast. Upon generation of the DL6 PN(s), the anterodorsal neuroblast apparently arrests, only producing additional projection neurons later in larval life (as indicated by heatshock-induced labeling of just a single anterodorsal glomerular class, DL1, until about 36 hours after larval hatching) (Jefferis et al., 2001).

In summary, embryonic-born PNs look just like larval-born PNs with regard to both their dendritic and axonal projections in the adult brain. Moreover, since their dendrites target a distinct subset of AL glomeruli and their axons exhibit characteristic terminal branching patterns in the LH according

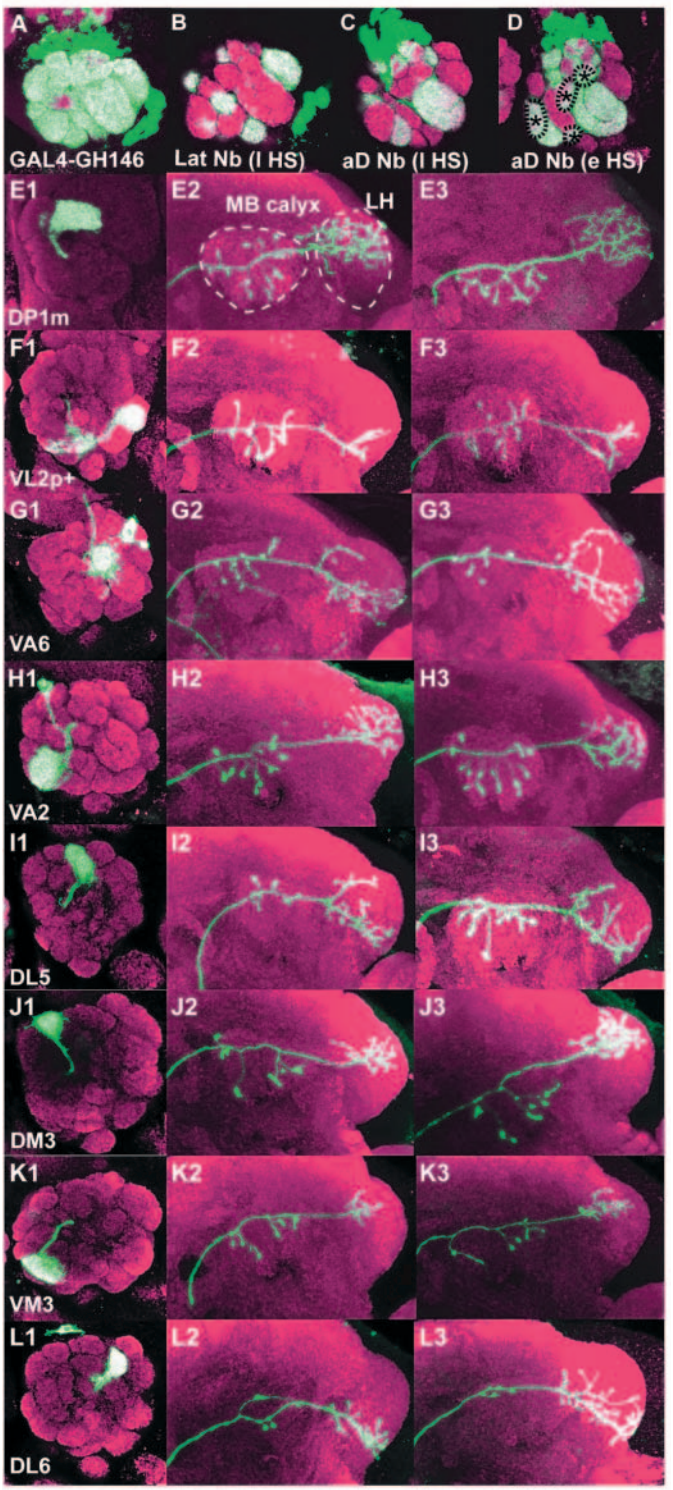

Fig. 1. Embryonic-born projection neurons exhibit characteristic connectivity in the adult olfactory system. (A-D) Many projection neurons innervating glomeruli in the adult AL are born during embryogenesis. (A) The GAL4-GH146 enhancer trap is expressed by ~90 PNs innervating approximately 40 of the ~50 glomeruli in the adult AL. (B) A lateral neuroblast clone labeled by early larval heatshock innervates 11 of these glomeruli. (C) An anterodorsal neuroblast clone labeled by early larval heatshock innervates a non-overlapping subset of 12 glomeruli. (D) An anterodorsal neuroblast clone labeled by early embryonic heatshock innervates at least 15 additional non-overlapping glomeruli. Asterisks indicate superficial glomeruli that are innervated by embryonic but not larval-born PNs. (E-L) Each embryonic-born PN generally innervates one glomerulus in adult AL (E1-L1) except VL2p+ (F1, see Table 1). Each glomerular class of PN exhibits a characteristic axon branching pattern in the MB calyx and LH (E2,E3-L2,L3 show two examples of each glomerular class). In this and subsequent figures, all brains were stained with anti-mCD8 (green, reporter for GAL4 or MARCM clones) and nc82 (magenta, marking neuropiles), and presented as flattened confocal stacks oriented with midline to the left and dorsal to the top unless otherwise noted. aD, anterodorsal; e HS, embryonic heatshock; GAL4-GH146, whole GH146 driver expression in AL; Lat, lateral; l HS, larval heatshock; Nb, neuroblast.

Table 1. Embryonic born PNs are prespecified to target dendrites to specific glomerulus by birth order

n	DP1m	VL2p*	VA6	VA2	DL5	DM3†	VM3‡	DL6§	DL1
2	–	–	–	–	–	–	–	–	+
11	–	–	–	–	–	–	–	+	+
6	–	–	–	–	–	–	+	+	+
8	–	–	–	–	–	+	+	+	+
6	–	–	–	–	+	+	+	+	+
10	–	–	–	+	+	+	+	+	+
19	–	–	+	+	+	+	+	+	+
3	–	+	+	+	+	+	+	+	+
8	+	+	+	+	+	+	+	+	+

n, the number of partial neuroblast clones that target dendrites to any of the nine glomeruli listed in the table.
*The VL2p PN usually also innervates VM4, but much more diffusely.
†DM3 appears to be somewhat variable and cannot be distinguished in every antennal lobe.
‡We identified one partial neuroblast clone in which DM3 was labeled but VM3 was not. However, in six cases, VM3 was labeled while DM3 was not, suggesting that VM3 was being innervated by PN(s) born after the one(s) that innervated DM3.
§Previously unreported, 'DL6' is a small, densely innervated glomerulus located just anterior to landmark glomerulus DL1.

to their glomerular classes, these embryonic-born PNs serve to expand the repertoire of odor representation in adults beyond the larval-born PNs previously characterized (Jefferis et al., 2001; Marin et al., 2002).

Embryonic-born projection neurons participate in the larval olfactory system

Given their early origin, these GH146-positive embryonic-born PNs may participate in the larval olfactory circuit as well. Indeed, examining third instar larval brains reveals that GH146 is strongly expressed in presumptive projection neurons that appear to innervate the larval AL and to send axons up to the MB calyx and larval equivalent of the adult LH (Fig. 2A) (Stocker et al., 1997). These projections appear to be contributed by about 16 to 18 clustered neurons that are presumably derived from the anterodorsal neuroblast.

To examine the morphology and connectivity of these PNs in the larval olfactory system with greater resolution, we used the MARCM method to specifically label PNs generated prior to larval hatching and dissected brains from wandering third instar larvae. In contrast to the larval-born PNs analyzed in earlier studies (Jefferis et al., 2004), all anterodorsal embryonic-born PNs exhibited densely branched dendrites in the larval AL and axons with large synaptic structures targeting glomerulus-like subregions in the MB calyx as well as branches in the presumptive LH (Fig. 2B). The large majority of the anterodorsal embryonic-born PNs each targeted a single glomerulus in the LAL (84%, *n*=70/83) (Fig. 2C1,C2) and/or in the MB calyx (71%, *n*=49/69) (Fig. 2D1,D2,E1,E2). In some cases, individual PNs targeted two glomeruli in one or both structures (Fig. 2C3,D3,E3). A more detailed analysis of the organizational logic of the larval olfactory circuit will be presented in a forthcoming manuscript (A. Ramaekers, E.

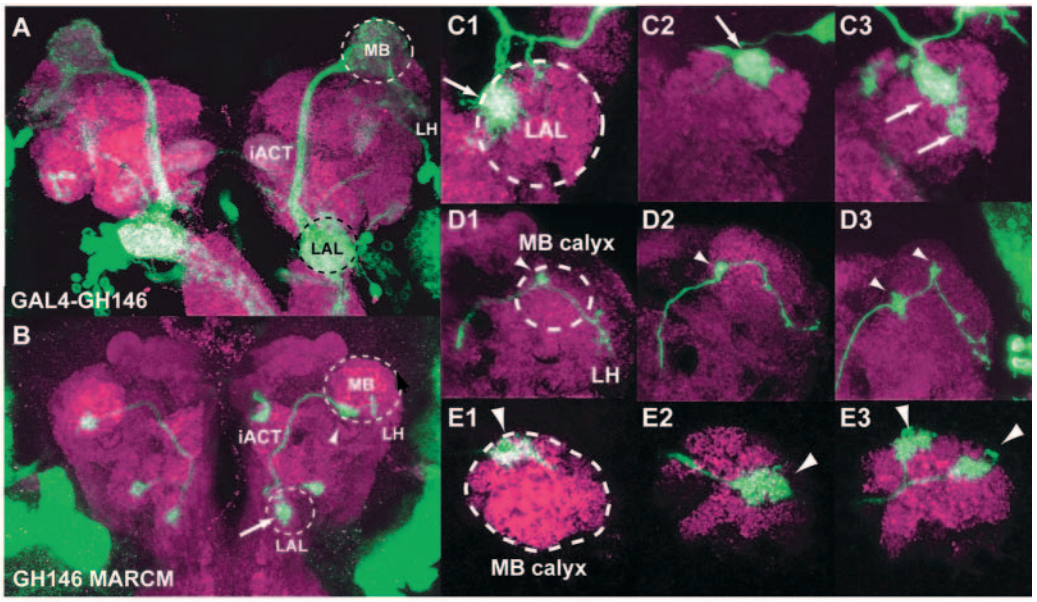

Fig. 2. Embryonic-born projection neurons participate in the larval olfactory system. (A) GAL4-GH146 staining pattern in the larval brain as visualized by UAS-mCD8-GFP reporter. PN dendrites innervate the larval AL and their axons travel via the inner and outer antennocerebral tracts to innervate ipsilateral higher brain centers, the MB calyx and the presumptive LH. (B) Single-cell clones of embryonic-born PNs (one on each hemisphere) show that each innervates one glomerulus in the larval AL and sends its axon to the MB calyx and LH. (C1-C3) High magnification of larval AL for three single-cell clones. Rarely, two glomerulus-like structures are innervated by a single PN (C3). (D1-D3) High magnification of axon projections for three single-cell clones. (E1-E3) Higher magnification of MB for three single-cell clones; each PN innervates one or occasionally two glomeruli in the larval MB calyx. Note: images C1-E3 are from nine different animals. Arrows indicate dendrites in larval AL glomeruli. Arrowheads indicate axon termini in MB calyx glomeruli. iACT, inner antennocerebral tract; LAL, larval antennal lobe.

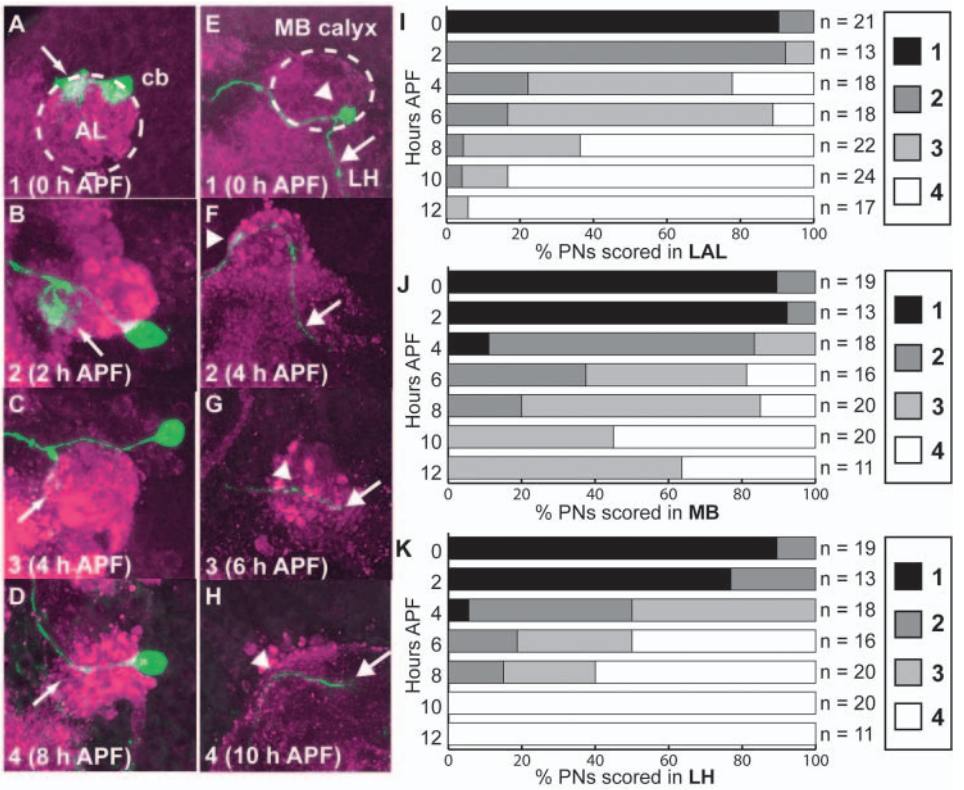

Fig. 3. Persistent projection neurons prune processes locally during early metamorphosis. (A-D) Timecourse for PPN dendritic pruning at the larval AL. (A) At the onset of puparium formation, each PPN labeled using GH146 MARCM has larval morphology, with dense dendrites in one glomerulus of the larval AL (score of 1). (B) As metamorphosis proceeds, dendrites in the larval AL start to disappear (score of 2). (C) Soon, only a few dendritic remnants are visible in the larval AL (score of 3). (D) Eventually, all dendritic remnants vanish from the larval AL (score of 4). (E-H) Timecourse for PPN axonal pruning at the larval MB and LH. (E) At puparium formation, each PPN has an axon with one or two large synaptic densities in MB calyx and branches in LH (score of 1). (F) The synaptic bouton in MB calyx shrinks as branches in the LH disappear (score of 2). (G) Soon only a slight swelling in the MB calyx indicates the former bouton and the main axon branch has begun to fragment (score of 3). (H) At last, no trace of the bouton(s) in MB calyx can be seen and the axon has pruned back to the edge of the MB calyx (score of 4). (I-K) Quantification of pruning scores of PPN dendrites in the (I) larval AL, (J) MB calyx and (K) LH every 2 hours APF. 0 hour APF brains were stained with anti-mCD8 and nc82, all others with anti-mCD8 and anti-synaptotagmin. Slender arrows indicate dendrites in the larval AL. Arrowheads indicate synaptic boutons in the MB calyx glomeruli. Blunt arrows indicate axon termini in the LH.

Magnenat, E.C.M., N. Gendre, G. Jefferis, L.L. and R. Stocker, unpublished).

Several lines of evidence suggest that the embryonic-born PNs observed in the larval olfactory system are the same cells as the PNs that contribute to the much larger and more complex adult circuit. First, the frequencies of labeled single-cell clones are comparable between the two stages, arguing against the possibilities that embryonic-born PNs are either dying off during metamorphosis or remaining quiescent and undetected through larval life. Second, the numbers of GH146-positive PNs observed at the time of puparium formation and in the adult are similar. Third, and most importantly, each embryonic-born PN undergoes characteristic morphological changes during metamorphosis, as described in detail below. Therefore, for the remainder of this paper, we will refer to the PNs labeled by embryonic heatshock as persistent projection neurons (PPNs), whether we are examining them in larva, pupa or adult. However, at this point, our methods do not allow us to correlate specific glomerular classes in larva with those observed later in adulthood.

Persistent projection neurons prune processes locally during early metamorphosis

How do PPNs participate in both larval and adult olfactory circuits? The larval and adult olfactory systems differ considerably in size and complexity, and at least some of the presumed synaptic partners of the PPNs, the MB γ neurons, are known to prune their processes during metamorphosis (Lee et al., 1999). Do PPNs remain essentially unaltered during metamorphosis, perhaps even providing cues for the pathfinding and/or targeting of later-born neurons? Or, like the MB γ neurons, do they prune their processes and then re-extend them to form new connections in the adult brain?

We have attempted live imaging of projection neurons during metamorphosis in intact pupae using two-photon microscopy; unfortunately, the brain is obscured by the opaque pupal cuticle and subcuticular fat. Our attempts to culture pupal brains outside of the cuticle with its complicated hormonal milieu have not yet been successful (D. Berdnik, A. Goldstein and L. Luo, unpublished). However, using MARCM to label PPNs and then dissecting brains every 2 hours after puparium formation (APF) permitted a series of developmental snapshots. This timecourse revealed that each PPN prunes its dendrites and axon terminals locally during early metamorphosis, leaving the main axon trunk from the cell body to the MB calyx intact, and later extends new processes to target the developing AL, MB and LH of the adult brain (Fig. 3).

To quantitatively analyze the pruning process and allow comparisons between wild-type and mutant animals, we assigned a score between 1 and 4 for the degree of pruning observed in each structure for a given sample. A score of 1 indicated that no difference from larval morphology could be discerned; a score of 2, that processes had become noticeably thinned; a score of 3, that processes were largely pruned but detectable remnants remained; and a score of 4, that all larval processes except for the main axon trunk from cell body to calyx had been eliminated. We summarize the timecourse

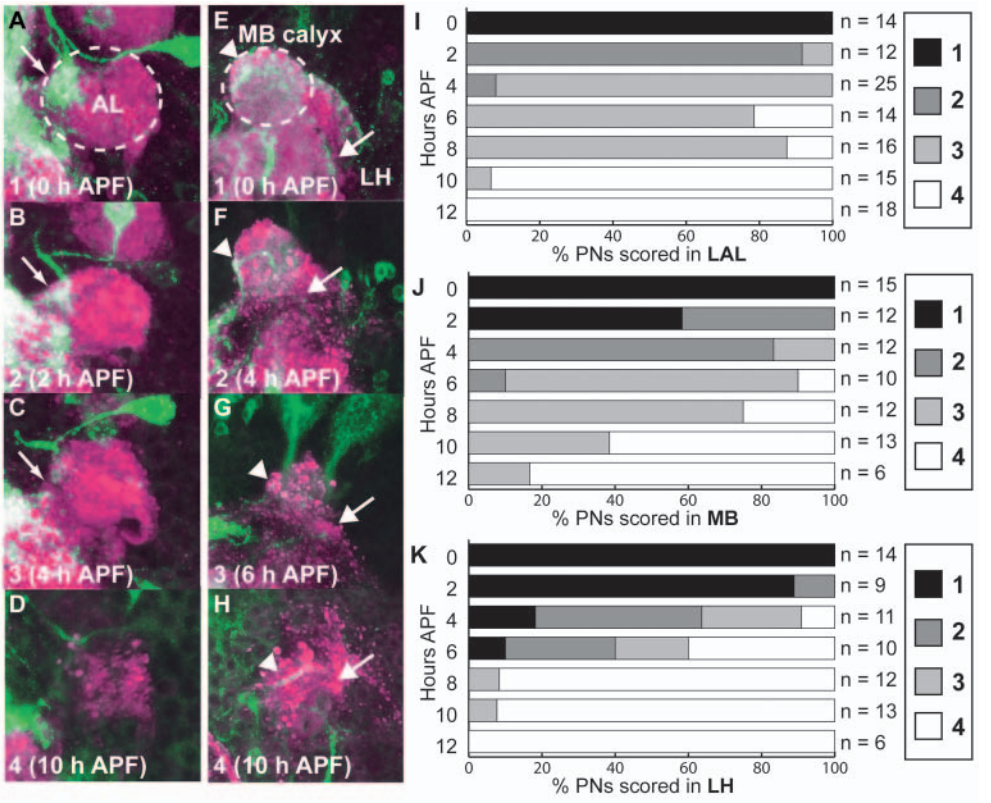

Fig. 4. MZ612+ persistent projection neurons prune processes locally during early metamorphosis. (A-H) Timecourse of pruning of (A-D) dendrites and (E-H) axons of the GAL4-MZ612-positive PPN. (I-K) Quantification of pruning scores of MZ612-positive PPN dendrites in the (I) larval AL, (J) MB calyx and (K) LH every 2 hours APF. Experimental conditions and figure labeling are as in Fig. 3. In addition to strongly labeling a single PPN that eventually innervates VA6 in adult, GAL4-MZ612 also labels other cells and processes near the larval AL, MB and LH. However, confocal tracing allows unambiguous distinction of PPN dendritic and axonal processes.

of PPN dendritic and axonal remodeling below.

PPN dendritic remodeling at larval AL

At the onset of puparium formation, PPN dendrites appear identical to those found in third instar larvae, with a large dendritic density clearly visible in the larval AL (score=1, Fig. 3A). But just 2 hours APF, dendrites in the larval AL appear thinned (score=2, Fig. 3B), and by 4 hours APF, they are mostly gone (score=3, Fig. 3C). In the next 4-8 hours, the larval dendritic processes are eliminated (Fig. 3I), while new filopodia start to appear from the main process more dorsally, in the presumed adult-specific AL (see Jefferis et al., 2004). By 18 hours APF, new dendrites have only begun to target specific regions of the newly forming adult-specific AL in two out of eight samples examined. This implies that embryonic-born PNs initiate innervation of the developing AL after the larval-born PNs, for which localized dendritic outgrowth is already visible by 6-12 hours APF (Jefferis et al., 2004).

PPN axonal remodeling at MB and LH

The axons of PPNs exhibit similar morphological changes, although beginning a little later in metamorphosis. For the first 2 hours APF, the majority of axons appear unchanged (score=1, Fig. 3E). By 4 hours APF, the presumptive synaptic structures in the MB calyx have become less dense, while the terminal branches in the larval LH are being pruned (score=2, Fig. 3F). Axon pruning proceeds over the next 6 hours until the main axon trunk terminates in the calyx, with no visible synaptic densities remaining (score=4, Fig. 3H). The remnants of PPNs in the calyx persist for a longer period of time compared to AL or LH (score=3, Fig. 3I-K), possibly reflecting the time it takes to turn over large presynaptic terminals there (see Fig. 5

Fig. 5. Ultrastructure analysis of MB calyx. (A) Ultrastructure analysis of larval (A2,A3) and 6 hours APF calyx (A4,A5) using GH146 driven EM marker CD2::HRP labeling PPN axons. (A1) Illustration of electron micrograph (EM) section plane using confocal Z projection of larval GH146-GAL4 driving mCD8::GFP, which labels the AL, inner antennocerebral tract and calyx with a dashed box showing the approximate location of EM section through the calyx. (A2) 4000× EM of the larval calyx showing the punctate labeling pattern with labeled boutons toward the outside of the calyx. Asterisks denote large presynaptic boutons. (A3) 40,000× EM of labeled larval PPN presynaptic terminals (filled arrowheads) apposing small unlabeled dendritic profiles postsynaptically. Open arrowheads point to the profile of the entire presynaptic bouton. (A4) 4000× EM of 6 hours APF degenerating PPN presynaptic boutons in the calyx. (A5) 40,000× EM at 6 hours APF with open arrowheads pointing to the border of a labeled presynaptic bouton and surrounding glia cytoplasm. (B) Ultrastructure analysis of larval (B2,B3) and 6 hours APF calyx (B4,B5) using GAL4-201Y driving CD2::HRP labeling MB γ neuron dendrites. (B1) Illustration of EM section plane using confocal Z projection of larval 201Y-GAL4 driving mCD8::GFP, which labels dendrites in the calyx, the axon peduncle, and medial and dorsal axon lobes. Dashed box shows approximate location of EM section through the calyx. (B2) 4000× EM of the larval calyx showing the concentric labeling pattern, with labeled dendrites toward the outside of the calyx. Asterisks denote large presynaptic boutons. (B3) 40,000× EM of labeled larval dendritic calyx showing unlabeled PPN presynaptic terminals (filled arrowheads) apposing small labeled dendritic profiles postsynaptically. (B4) 4000× EM of 6 hours APF MB γ neuron labeled calyx showing degeneration of larval concentric labeling. (B5) 40,000× EM at 6 hours APF with an arrow specifying a degenerating synapse full of synaptic vesicles surrounded by labeled dendritic profiles, which appear to be engulfed by a glia (open arrowheads pointing to the border of engulfed synaptic profiles and glia cytoplasm). Dotted lines in A2,A4,B2,B4 denote the border of the calyx. Scale bars: 50 μm in A1,B1; 10 μm in A2,A4,B2,B4; 1 μm in A3,A5,B3,B5. c, calyx; d, dorsal axon lobe; iACT, inner antennocerebral tract; m, medial axon lobe; p, axon peduncle.

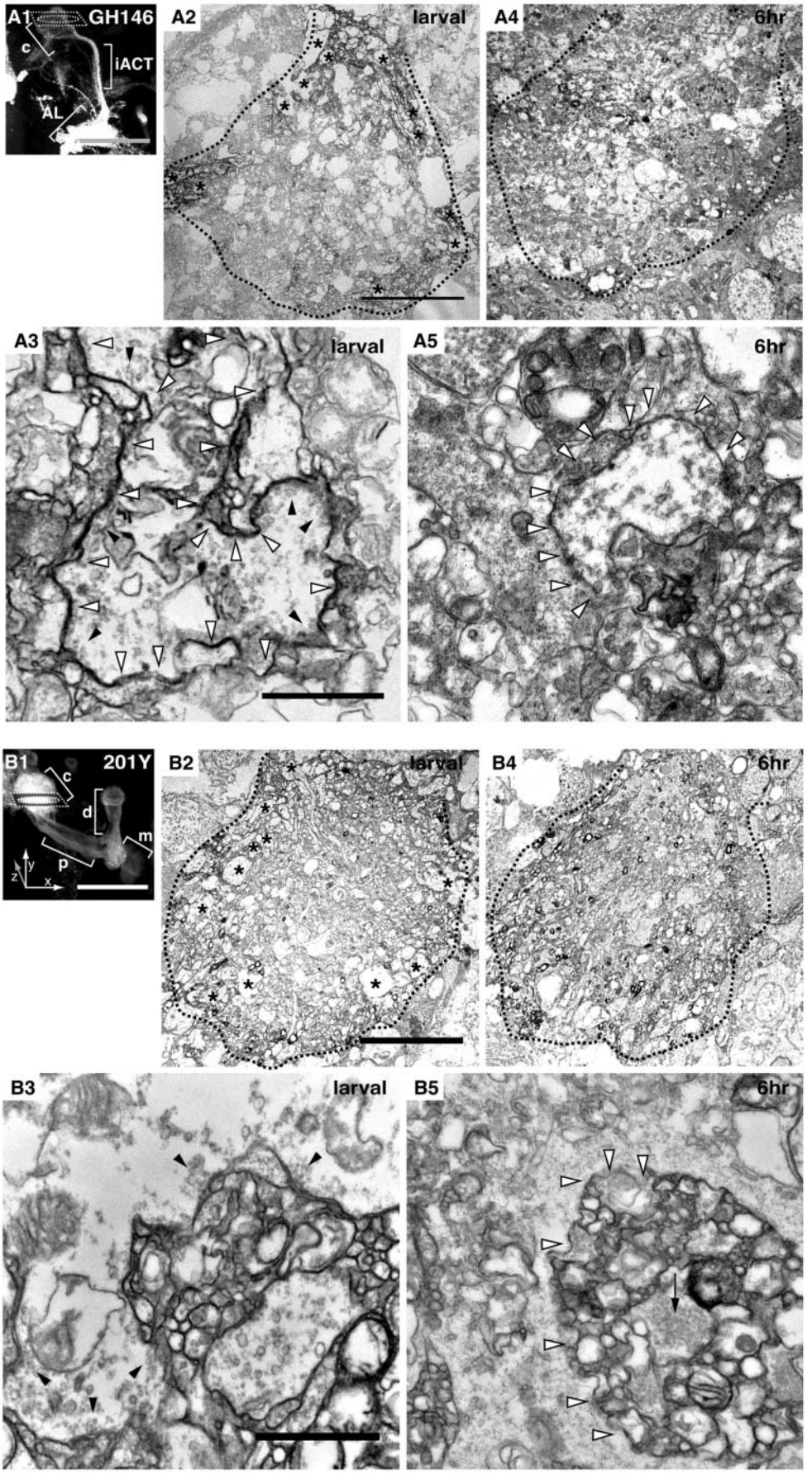

below). Although fine filopodia sometimes can be seen to extend from the end of the axon, no directed outgrowth is observed through 12 hours APF. However, exuberant new processes re-extend into both the calyx and the LH region by 18 hours APF in seven of eight samples examined.

Although there was some temporal variability, all PPNs examined appeared to undergo a similar process of reorganization during the first 18 hours of metamorphosis (Fig. 3I-K). The observed variation might be due to small differences in developmental status at the time of white pre-pupa collection and/or differences in developmental rates between animals after the initial staging. Another possibility is that different glomerular classes of PPNs exhibit slightly different characteristic rates of reorganization that have been obscured by pooling developmental data from the entire population of GH146-positive PPNs.

To determine whether the latter possibility might indeed be the case, we made use of a second, more specific, projection neuron driver, GAL4-MZ612. This driver is strongly expressed by one PPN innervating glomerulus VA6 in the adult antennal lobe, previously identified by GH146 MARCM as an embryonic-born PN target (Fig. 1G). It also strongly labels one PN in the larval olfactory circuit, which innervates a medial glomerulus in the larval AL. MZ612-based MARCM experiments confirm that this neuron is labeled by inducing recombination during embryogenesis and that it persists to innervate VA6 in the adult.

Just like the GH146-positive PPNs, the MZ612-positive neuron prunes and then re-extends its processes in the first 18 hours after metamorphosis (Fig. 4A-H). Interestingly, the timecourse of reorganization appeared less variable for this homogeneous population of PPNs (Fig. 4I-K, compare with Fig. 3I-K). This supports the idea that at least

some of the variation observed for the GH146-positive PNs was attributable to characteristic differences in pruning dynamics between glomerular classes.

Synapse disassembly visualized by electron microscopy

To visualize PPN pruning with higher resolution, we took advantage of a recently developed method that allowed us to examine identifiable neuronal elements in electron micrographs (Watts et al., 2004). We focused our study on the MB calyx as both presynaptic (PPN axons; Figs 3, 4) and postsynaptic (MB γ neuron dendrites) (Lee et al., 1999; Watts et al., 2003) elements undergo pruning during early metamorphosis. A genetically encoded electron micrograph marker, HRP::CD2, was expressed by either GAL4-GH146 (Fig. 5A) to label PPN axon terminals or GAL4-201Y (Fig. 5B) to label MB γ neuron dendrites. Electron micrographs were taken in the orientation illustrated by the fluorescence images (Fig. 5A1,B1).

Electron micrographs from wandering third instar larvae in which HRP::CD2 was driven by GH146 (Fig. 5A2,A3) or 201Y (Fig. 5B2,B3) gave complementary results supporting the following model. Persistent projection neuron axon terminals appear as large presynaptic boutons (2-4 μm in size; * in Fig. 5A2,B2) that contain synaptic vesicles apposing postsynaptic profiles (arrowheads in Fig. 5A3,B3). These structures are enriched in the peripheral calyx and probably correspond to glomerulus-like structures seen with fluorescence microscopy (Fig. 2E1-E3), analogous to the 'calycal glomerulus' described in adult calyx (Yasuyama et al., 2002). Only a subset of these large presynaptic boutons is labeled by GH146, consistent with the fact that only a subset of PPNs are GH146-positive. MB γ neuron dendritic profiles are small and numerous (labeled in Fig. 5B3), and are directly postsynaptic to large profiles of presynaptic boutons presumed to be from PNs. These experiments therefore provide direct morphological evidence that PPN axons form functional synapses in the larval circuit with dendrites of MB γ neurons.

At 6 hours APF, the peak of MB γ neuron dendrite pruning (Watts et al., 2003) and PPN axon pruning (Fig. 3), electron microscopy analyses of calyx labeled with PPNs (Fig. 5A4,A5) or MB γ neurons (Fig. 5B4,B5) revealed that the large presynaptic boutons have been disassembled. Both PPN synaptic terminals and MB γ neuron dendritic profiles appear to be engulfed by glia (Fig. 5A5,B5, open arrowheads; glial profiles were identified by characteristic glycogen granules), as has been shown recently for MB γ neuron axons (Watts et al., 2004).

Requirement of ecdysone co-receptor and TGFβ receptor for PPN pruning

Prior studies have used MB γ neurons as a model system to study the molecular mechanisms of axon pruning. γ neuron pruning depends on cell-autonomous reception of the steroid hormone ecdysone; single neurons that are homozygous mutant for the ecdysone co-receptor *ultraspiracle* (*usp*) in an otherwise heterozygous brain fail to reorganize their processes and retain both dorsal and medial axon lobes in the adult brain (Lee et al., 2000). In addition, γ neurons must upregulate the expression of ecdysone receptor isoform B1 (EcRB1) prior to axon pruning (Lee et al., 2000). This upregulation requires TGFβ signaling, as MB γ neurons that are mutant for the TGFβ/Activin Type I receptor *baboon* (*babo*) or its downstream effector *Dsmad* do not upregulate EcRB1 expression and consequently fail to prune (Zheng et al., 2003).

We asked whether a similar molecular pathway is utilized during PPN reorganization. To ascertain whether the pruning of PPNs is also regulated by ecdysone, we first examined EcRB1 expression patterns. At puparium formation, only 20 of the ~90 GH146+ projection neurons present were strongly positive for EcRB1. These strongly stained PNs, ~18 of which belonged to the anterodorsal cluster, also had noticeably larger and brighter cell bodies than surrounding PNs, which were probably immature larval-born PNs (n=10/10). Single-cell MARCM clones generated by embryonic heatshock were also strongly positive for EcRB1 at puparium formation (Fig. 6A1, n=10/10). Thus, we conclude that EcRB1 expression is highly expressed in PPNs at the onset of metamorphosis.

Is TGFβ signaling generally required to regulate expression of EcRB1 for neuronal pruning during metamorphosis? We used MARCM to label cells that were homozygous for the strongest *baboon* allele, $babo^{Fd4}$, in a heterozygous background to test whether PPNs also require TGFβ reception for normal pruning. At the wandering third instar stage, PPNs homozygous for $babo^{Fd4}$ appeared to have normal dendritic and axonal projections (Fig. 6B2,C2; n=7/7). However, $babo^{Fd4}$ PPNs failed to show high-level expression of EcRB1 by the onset of puparium formation (Fig. 6A2; n=8/8). This result indicates that, as for the MB γ neurons, high-level expression of EcRB1 in remodeling PPNs depends on TGFβ signaling.

Consistent with the loss of EcRB1 expression, $babo^{Fd4}$ PPNs failed to reorganize their processes normally during the first few hours of metamorphosis. For wild-type PPNs at 8 hours APF, approximately 95% of dendrites, 80% of MB calyx processes, and 85% of LH processes are in the final two stages of pruning (Fig. 6F). However, most of the embryonic-born $babo^{Fd4}$ PPNs still retained dendrites and axons with larval morphology at this time (Fig. 6F). Dense dendritic processes were visible in the larval AL for 100% of PN clones examined (Fig. 6D2,F), and only 14% of axon branches in the LH appeared to resemble the final two stages of pruning (Fig. 6E2,F). The degree of pruning in the calyx was more difficult to estimate, due to the concurrent degeneration of γ MB neuron dendrites and loss of glomerular organization, but disappearance of synaptic boutons still seemed inhibited (Fig. 6E2,F).

To confirm that this failure to prune resulted from loss of ecdysone signal reception, we also used MARCM to label PPNs that were homozygous for a well-characterized mutant allele (Lee et al., 2000) of the ecdysone co-receptor, usp^3. At the wandering third instar stage, usp^3 PPNs exhibit normal morphology (Fig. 6B3,C3; n=17/17), and, as expected, EcRB1 was expressed at wild-type levels at the time of puparium formation (Fig. 6A3; n=10/10).

However, when we examined these brains at 8 hours APF, we observed a significant defect in dendrite and axon pruning. In the majority of cases, both dendritic densities in the location of the larval antennal lobe (Fig. 6D3) and axon branches in the MB calyx and LH had been retained (Fig. 6E3, quantified in Fig. 6F). Taken together, these mosaic experiments suggest that PPN dendritic and axonal pruning require cell-autonomous

function of EcRB1/USP, as has been shown previously for MB γ neurons.

Adult phenotypes for PPNs defective in pruning

What are the consequences for the adult olfactory circuit when larval circuits fail to prune? PPNs homozygous for *usp*^{3} or *babo*^{Fd4} that failed to prune their dendrites and axons during metamorphosis allowed us to investigate this question.

When examined in adults, wild-type PPN dendrites were confined to a single glomerulus in the adult AL with the exception of the VL2p+ class (Fig. 1; Fig. 7A1). Dendrites of single-cell PPN clones homozygous for *usp*^{3} generally appeared to target glomeruli in the adult AL appropriate for PPNs; however, ectopic processes in additional areas of the AL (arrows in Fig. 7B1,B2; quantified in Fig. 7G), which could be interpreted as persisting larval dendrites, were often present. In a few cases, *usp*^{3} PPN dendrites were sparser and less specifically targeted to particular glomeruli, but still remained somewhat confined to certain regions of the AL (quantified in Fig. 7G). Likewise, whereas wild-type PPNs always exhibited terminal swellings on short side branches (Fig. 1; Fig. 7A2), about 40% of *usp*^{3} PPNs retained larval-like boutons directly on their main trunks in the MB calyx (arrowheads in Fig. 7B2,C2); however, they always had side branches with terminal swellings as well, implying that re-extension and adult-specific outgrowth were not completely impaired. In addition, the main axon trunk often diverted conspicuously from the inner antennocerebral tract in the MB calyx, presumably to maintain contact with the larval boutons (Fig. 7C2). Nearly all *usp*^{3} PPN axons exhibited grossly wild-type morphologies in adult LH; only one *usp*^{3} PPN axon in our sample failed to enter the LH. In summary, *usp*^{3} PPNs display ectopic processes in AL and MB that appear to be due to defects in pruning during early metamorphosis; these pruning defects do not seem to interfere with the growth or even targeting (in the case of AL) of adult-specific processes.

In comparison, *babo*^{Fd4} PPNs exhibited more severe dendritic and axonal phenotypes in the adult brain (Fig. 7G-I). In a few cases, these PPNs had targeted an appropriate glomerulus but also featured ectopic processes. More commonly, we observed sparse diffuse processes in the AL that were somewhat localized but did not appear to target any specific glomerulus (Fig. 7D1). Processes also occasionally strayed to arborize outside the ventral AL (Fig. 7E1). In the most severe cases, sparse dendrites were distributed broadly throughout the AL (Fig. 7F1). In the MB calyx, all *babo*^{Fd4} PPN axons appeared to have retained large larval-like boutons

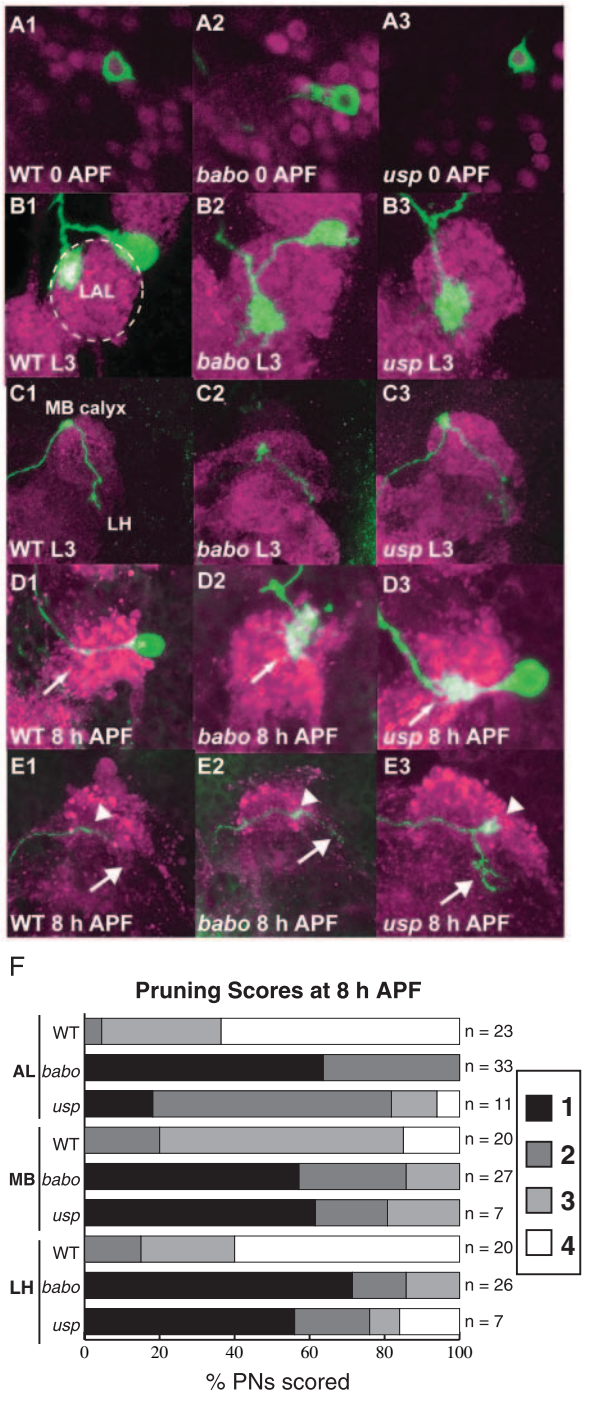

Fig. 6. Persistent projection neuron pruning requires *ultraspiracle* and *baboon*. Anti-EcR-B1 staining (magenta) in single-cell MARCM clones (green) that are (A1) wild-type or homozygous for (A2) *babo*^{Fd4} or (A3) *usp*^{3}. At the onset of puparium formation, (A2) *babo*^{Fd4} PPNs fail to express EcRB1, as indicated by the lack of nuclear magenta in the MARCM single-cell clone. At third instar larva, single-cell MARCM clones of PPNs homozygous for (B2) *babo*^{Fd4} or (B3) *usp*^{3} exhibit apparent normal dendritic projections in larval AL compared with (B1) wild-type control. At third instar larva, single-cell MARCM clones of PPNs homozygous for (C2) *babo*^{Fd4} or (C3) *usp*^{3} exhibit apparent normal axonal projections in larval MB and LH compared with (C1) wild-type control. At 8 hours APF, (D1) the majority of wild type PPNs have completely pruned their dendrites in the larval AL. However, many (D2) *babo*^{Fd4} and (D3) *usp*^{3} PPNs still exhibit larval-like dense dendrites in the larval AL. At 8 hours APF, the majority of wild-type PPNs have largely eliminated their boutons in the MB calyx and pruned their axons back to the edge of the calyx (E1). By contrast, most (E2) *babo*^{Fd4} and (E3) *usp*^{3} PPN axons still retain larval-like morphology, with large boutons in the MB calyx and terminal branches in the LH. (F) Cumulative pruning scores in larval AL, MB calyx and LH at 8 hours APF. L3 brains were stained with anti-mCD8 and nc82. At 8 hours APF, brains were stained with anti-mCD8 and anti-synaptotagmin. Slender arrows indicate dendrites in larval AL. Arrowheads indicate synaptic boutons in MB calyx glomeruli. Blunt arrows indicate axon termini in LH. L3, third instar larva; LAL, larval antennal lobe; WT, wild type.

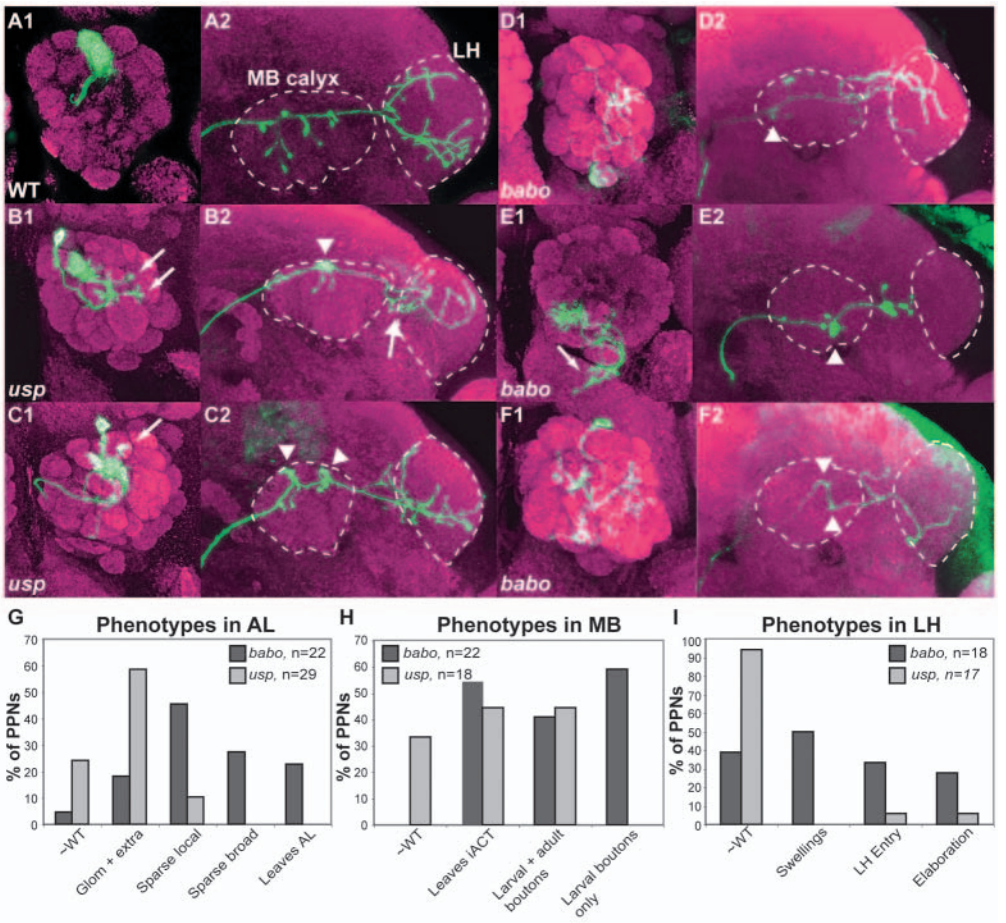

Fig. 7. Adult phenotypes of *ultraspiracle* and *baboon* PPN clones. (A1) Wild-type PPNs labeled by GH146 MARCM typically innervate a single glomerulus in the adult AL and (A2) have several collateral branches with terminal boutons in the MB calyx and a characteristic branching pattern in the LH (see also Fig. 1). (B1,C1) usp^3 PPN dendrites generally target an appropriate glomerulus in the AL but also exhibit a few ectopic processes (arrows), while (B2,C2) their axons often retain large larval-like synaptic structures directly on the main trunk (arrowheads). The axon trunk sometimes makes a detour from the main inner antennocerebral tract within MB to connect these larval-like boutons (C2 only). Axon termini in the LH are morphologically normal, although they may include possible extra branches, which might be putative larval remnants (B2, blunt arrow). (D1-F1) $babo^{Fd4}$ PPN dendrites often exhibit more severe phenotypes than that of usp^3; they can be sparse and localized to a few areas in the AL without targeting a specific glomerulus (D1), leave the AL entirely (E1, arrow), or be broadly distributed throughout the AL (F1). (D2-F2) All $babo^{Fd4}$ PPN axons exhibit larval-like boutons directly on their main trunks in the MB calyx (arrowheads) and occasionally detour from the inner antennocerebral tract to connect them (F2 only). Additional defects seen in the LH include unusually profuse swellings along the branches (D2), failure to enter the LH (E2), and failure to elaborate axon termini (F2). Note: All AL and MB/LH images are presented in pairs from the same animal, but this is not meant to imply consistent correlations between the various dendritic and axonal phenotypes. (G) Quantification of usp^3 and $babo^{Fd4}$ phenotypes in the adult AL. Categories are '~WT' (uniglomerular dense dendrites), 'glom + extra' (uniglomerular dendrites plus extra processes in the AL), 'sparse local' (sparse dendrites localized to a region of the AL but not innervating any particular glomerulus), 'sparse broad' (sparse dendrites distributed broadly throughout the AL) and 'leaves AL' (dendrites arborize outside the AL proper). Note that although the first four categories are mutually exclusive, the fifth can overlap with any of the others except for '~WT'. (H) Quantification of usp^3 and $babo^{Fd4}$ phenotypes in the adult MB calyx. Categories are '~WT' (adult-like collateral branches with terminal swellings), 'leaves iACT' (main axon trunk detours from the inner antennocerebral tract, usually to connect with a larval-like bouton), 'larval + adult boutons' (both larval-like boutons on the main axon trunk and adult-like collateral branches), and 'larval boutons only' (larval-like boutons on the main axon trunk but no adult-like collateral branches). Note that 'leaves iACT' can overlap with either of the last two categories; the others are mutually exclusive. (I) Quantification of usp^3 and $babo^{Fd4}$ phenotypes in the adult LH. Categories are '~WT' (terminal branches of varying complexity in LH), 'swellings' (unusually profuse swellings along the terminal branches), 'LH entry' (failure to enter the LH proper), and 'elaboration' (failure to elaborate second order terminal branches in the LH). Note that there is overlap between all categories except for '~WT'.

directly on their main trunks, rather than exclusively terminal swellings on short side branches as in wild type (arrowheads in Fig. 7D2,E2,F2); in 64% of cases, there were no MB collaterals with wild-type adult appearance at all (Fig. 7F2). The main axon trunk often diverged dramatically from the inner antennocerebral tract in the MB calyx (Fig. 7F2). Finally, in the LH, the majority of $babo^{Fd4}$ PPNs featured significant aberrations including unusually profuse swellings along the branches (Fig. 7D2), failure to enter the LH (Fig. 7E2) and/or failure to elaborate higher order branches in the LH (Fig. 7F2). These phenotypes imply an axon re-extension, pathfinding and/or targeting defect in addition to the impaired pruning observed at 8 hours APF.

In summary, both usp^3 and $babo^{Fd4}$ PPNs exhibit phenotypes in the adult brain consistent with blockage of pruning during early metamorphosis, including extraglomerular processes in the AL as well as large larval-like boutons on the main trunk and diversion from the inner antennocerebral tract as the axon passes through the MB calyx. However, $babo^{Fd4}$ PPNs also feature more severe phenotypes, particularly a complete lack of glomerular innervation and of adult-like axon collaterals with terminal swellings in the MB calyx, as well as failure to enter the LH and/or to elaborate higher order terminal branches. These latter phenotypes appear to be qualitatively different from those attributable to a simple loss of pruning, suggesting that TGFβ signaling via *baboon* may have an

additional role in re-extension and/or adult-specific targeting during metamorphosis.

Discussion

In this study, we have shown that the PPNs of the *Drosophila* olfactory system play analogous functions in two neural circuits at different life stages. They do so by developmentally programmed disassembly and reassembly of synaptic connections during metamorphosis. We discuss below the implications of our findings for the larval and adult olfactory systems and to neural circuit reorganization.

PPNs function in both larval and adult olfactory circuits

We have shown that PPNs serve as relay interneurons connecting the antennal lobe to the MB calyx and the presumptive LH in larvae, just as previously characterized larval-born projection neurons do in adults. Each PPN generally targets its dendrites to one glomerular substructure in the larval AL, probably receiving input from one of the 21 olfactory receptor neurons of the dorsal organ. From there, the PPN's axon extends to higher brain centers, forming one or two large synaptic structures en passant on its way through the MB calyx to the LH. Our electron microscopy studies with genetically encoded markers expressed separately in PPNs or in MB γ neurons established that PPNs form functional synapses in the larval circuit and that MB γ neurons are among their postsynaptic partners.

Our analysis of these PPNs in the adult olfactory circuit confirmed and extended the developmental and wiring logic derived from our previous analysis of larval-born PNs. Just like larval-born PNs (Jefferis et al., 2001), embryonic-born PPNs are prespecified to target their dendrites to particular glomeruli according to their birth order. Specifically, most PPNs are derived from the same anterodorsal neuroblast that later gives rise to about half the GH146-positive PNs. Like the larval-born PNs (Marin et al., 2002), PPNs exhibit stereotyped terminal arborization patterns in the LH (see also Wong et al., 2002). Interestingly, in the adult AL, PPNs innervate a distinct subset of glomeruli from either their larval-born anterodorsal cousins or the projection neurons generated by the lateral neuroblast. This indicates that, in addition to relaying activity from larva-specific olfactory receptor neurons earlier in development, PPNs expand the olfactory repertoire of the adult circuit.

As odorant response profiles of individual ORs are systematically mapped (Dobritsa et al., 2003; Hallem et al., 2004), and glomerular projection patterns of individual ORN classes are determined in both the adult (e.g. Komiyama et al., 2004; Vosshall et al., 2000) and in the larval antennal lobe in the future, it will be extremely interesting to compare whether these PPNs represent similar or distinct odor repertoires at different life stages. At this point, one could speculate that the PPNs represent odors that possess ethological significance for both larvae and adult flies, perhaps by forming adult-specific connections with ORNs expressing the same olfactory receptors found in larvae. However, PPNs may be collectively no different from the larval-born PNs in the adult olfactory system and may simply follow the same rules of connectivity previously suggested, with PNs that innervate neighboring glomeruli in the AL also targeting similar regions of the LH (Marin et al., 2002).

Implications for the development of the adult olfactory circuit

In addition to serving larval-specific functions, one proposed function for larval circuits is to provide a foundation upon which adult circuits can be built. In the case of the olfactory circuit, however, our previous analysis indicated that the adult-specific antennal lobes form adjacent to, but spatially distinct from, the larval antennal lobe (Jefferis et al., 2004). Our analysis of PPN remodeling supports the notion that the adult circuit is constructed de novo rather than upon the larval circuit. A developmental timecourse analysis revealed that PPNs prune their dendrites and axon branches during early metamorphosis, so that only the main unbranched process from the cell body to the distal edge of the calyx remains by 12 hours APF (Fig. 3). By contrast, the larval-born PNs begin to elaborate dendrites at the onset of puparium formation and restrict their processes to specific regions of the developing AL between 6 and 12 hours APF (Jefferis et al., 2004). Persistent projection neurons start exhibiting this type of localized dendritic outgrowth in the adjacent but distinct adult AL site only at 18 hours APF, around the time that adult-specific ORN axons arrive but prior to their invasion of the AL. This strongly implies that, far from providing contact-mediated cues for differentiating larval-born PNs, PPNs target glomeruli in the developing AL only after the larval-born PNs have established their dendritic target domains. The finding that PPN-specific glomeruli are intercalated with those targeted by dendrites of larval-born PNs, rather than occupying a spatially segregated domain in the adult antennal lobe, implies complex targeting rules in the establishment of wiring specificity of the adult circuit.

Relationship between pruning and re-extension

The fact that PPNs have clearly identifiable addresses for their dendritic targeting in the adult circuit allowed us to ask the interesting question: does assembly of the adult circuit depend on the disassembly of the larval circuit? Our data suggest that neuronal reorganization appears to be separable into two at least partially independent events, pruning and re-extension. Even usp^3 PPNs whose larva-specific dendrites and axons appear unpruned still exhibit the random fine filopodial extensions characteristic of wild-type neurons at 8-12 hours APF (data not shown), and moreover target their new dendrites to appropriate adult antennal lobe glomeruli, as well as exhibiting adult-specific axon collaterals in the MB calyx and grossly wild-type terminal branches in the LH (Fig. 7).

The fact that most usp^3 persistent PNs still innervate appropriate glomeruli in the adult antennal lobe and have axons with adult characteristics would suggest that *ultraspiracle*-mediated execution of ecdysone signaling is required for pruning but not for responding to re-extension and/or targeting cues in the developing brain. However, most $babo^{Fd4}$ PPNs failed to target appropriately in the adult olfactory system. This difference in phenotypes may be due to differential perdurance of wild-type Usp versus Babo protein in single-cell MARCM clones and/or to differences in the severity of the alleles examined, consistent with the observation that $babo^{Fd4}$ PPNs show slightly more homogeneous pruning phenotypes at 8

hours APF (Fig. 5F). However, *usp*^{3} carries a missense mutation that alters an invariant arginine in the DNA-binding domain and blocks MB γ neuron pruning completely (Lee et al., 2000). Thus, we favor the possibility that *baboon* is required for additional *ultraspiracle*-independent functions during metamorphosis, in the initiation of pruning, re-extension and/or targeting of adult olfactory structures.

Regulation of neural circuit remodeling during metamorphosis

Since the original description of dendritic remodeling in an identified *Manduca* motoneuron during metamorphosis (Truman and Reiss, 1976), neuronal remodeling during insect metamorphosis has been extensively studied, in particular for motoneurons of *Manduca* and *Drosophila* (reviewed by Levine et al., 1995; Tissot and Stocker, 2000). Most of these studies have been conducted in individual identified neurons. Our study of PPN remodeling reported here, in conjunction with previous studies of MB γ neurons that we have shown to be postsynaptic targets of PPNs (Fig. 5), offers a unique opportunity to examine how synaptic partners coordinate their remodeling.

We find that within each individual class of neurons, the timing of axon and dendrite pruning are not necessarily synchronized. For instance, MB γ neurons prune their dendrites (4-8 hours APF) prior to their larval-specific axon branches (6-18 hours APF) (Watts et al., 2003). Likewise, PPNs prune their dendrites (2-6 hours APF) slightly before axon terminals in MB and LH (4-12 hours APF). However, pruning of PPN axon terminals and MB γ neuron dendrites in the calyx appears to be coincident, raising the possibility that the pruning of synaptic partners might be coordinated, or might even influence one another.

However, genetic studies indicate that there is at least some degree of independence between these partner neurons. Given that remodeling occurs during metamorphosis, regulation by the steroid hormone ecdysone had been strongly implicated (Levine et al., 1995). Earlier studies in *Manduca* using surgical and endocrinological manipulations revealed that muscle degeneration and motoneuron dendritic pruning and death are independently regulated by edcysone (Weeks and Truman, 1985). Genetic tests for cell-autonomy had been performed using single-cell mutant and cell-type-specific rescue analysis in MB neurons (Lee et al., 1999) and peptidergic Tv neurons (Schubiger et al., 2003). In most other cases it has not been unequivocally determined whether ecdysone acts directly on the remodeling neurons, or whether some of the effects of ecdysone could be exerted indirectly through the environment, including their synaptic partners. Single-cell clone analyses using *babo* or *usp* mutants in this study strongly suggested that ecdysone also acts directly on each individual PPN to regulate axon and dendrite pruning. Thus, PPN axon pruning in MB calyx cannot be entirely a consequence of pruning of its postsynaptic partners, just as MB γ neuron dendrite pruning cannot be entirely a consequence of pruning of its presynaptic partners. Rather, they are developmentally programmed independently, although, interestingly, they use the same mechanisms involving TGF-β induced expression of EcR-B1, which works together with its co-receptor Usp to regulate gene expression.

These experiments by no means exclude the possibility that PN axon pruning and MB γ neuron dendrite pruning are to some degree interdependent. For instance, it could be that ecdysone signaling confers competence to prune on each class of neurons, but the execution of the pruning process would depend on further cellular interactions, including those between synaptic partners. Future genetic manipulations that block pruning of one class of neurons and examine the consequences for the other class will shed light on the contribution of cellular interactions in neural circuit remodeling.

We thank M. Metzstein, M. Krasnow, T. Lee, E. Buchner, H. Bellen and C. Thummel for reagents, G. Jefferis for the initial observations regarding embryonic-born PNs, and J. Perrino of the Stanford EM facility for technical help. We also thank S. Rafelski for advice on quantification and R. Stocker, S. McConnell, G. Jefferis and D. Manoli for comments on drafts of the manuscript. E.C.M. was supported by an HHMI pre-doctoral fellowship. This work was supported by an NIH grant (NS41044) to L.L.

References

Armstrong, J. D., de Belle, J. S., Wang, Z. and Kaiser, K. (1998). Metamorphosis of the mushroom bodies; large-scale rearrangements of the neural substrates for associative learning and memory in *Drosophila*. *Learn. Mem.* **5**, 102-114.

Awasaki, T. and Ito, K. (2004). Engulfing action of glial cells is required for programmed axon pruning during Drosophila metamorphosis. *Curr. Biol.* **14**, 668-677.

Clyne, P. J., Warr, C. G., Freeman, M. R., Lessing, D., Kim, J. and Carlson, J. R. (1999). A novel family of divergent seven-transmembrane proteins: candidate odorant receptors in Drosophila. *Neuron* **22**, 327-338.

Cobb, M. and Domain, I. (2000). Olfactory coding in a simple system: adaptation in Drosophila larvae. *Proc. R. Soc. London B Biol. Sci.* **267**, 2119-2125.

Dobritsa, A. A., van der Goes van Naters, W., Warr, C. G., Steinbrecht, R. A. and Carlson, J. R. (2003). Integrating the molecular and cellular basis of odor coding in the Drosophila antenna. *Neuron* **37**, 827-841.

Gao, Q. and Chess, A. (1999). Identification of candidate Drosophila olfactory receptors from genomic DNA sequence. *Genomics* **60**, 31-39.

Gao, Q., Yuan, B. and Chess, A. (2000). Convergent projections of Drosophila olfactory neurons to specific glomeruli in the antennal lobe. *Nat. Neurosci.* **3**, 780-785.

Hallem, E. A., Ho, M. G. and Carlson, J. R. (2004). The molecular basis of odor coding in the Drosophila antenna. *Cell* **117**, 965-979.

Heimbeck, G., Bugnon, V., Gendre, N., Haberlin, C. and Stocker, R. F. (1999). Smell and taste perception in Drosophila melanogaster larva: toxin expression studies in chemosensory neurons. *J. Neurosci.* **19**, 6599-6609.

Jefferis, G. S., Marin, E. C., Stocker, R. F. and Luo, L. (2001). Target neuron prespecification in the olfactory map of Drosophila. *Nature* **414**, 204-208.

Jefferis, G. S., Vyas, R. M., Berdnik, D., Ramaekers, A., Stocker, R. F., Tanaka, N. K., Ito, K. and Luo, L. (2004). Developmental origin of wiring specificity in the olfactory system of Drosophila. *Development* **131**, 117-130.

Komiyama, T., Carlson, J. R. and Luo, L. (2004). Olfactory receptor neuron axon targeting: intrinsic transcriptional control and hierarchical interactions. *Nat. Neurosci.* **7**, 819-825.

Lee, T. and Luo, L. (1999). Mosaic analysis with a repressible cell marker for studies of gene function in neuronal morphogenesis. *Neuron* **22**, 451-461.

Lee, T., Lee, A. and Luo, L. (1999). Development of the *Drosophila* mushroom bodies: sequential generation of three distinct types of neurons from a neuroblast. *Development* **126**, 4065-4076.

Lee, T., Marticke, S., Sung, C., Robinow, S. and Luo, L. (2000). Cell-autonomous requirement of the USP/EcR-B ecdysone receptor for mushroom body neuronal remodeling in Drosophila. *Neuron* **28**, 807-818.

Levine, R. B., Morton, D. B. and Restifo, L. L. (1995). Remodeling of the insect nervous system. *Curr. Opin. Neurobiol.* **5**, 28-35.

Marin, E. C., Jefferis, G. S., Komiyama, T., Zhu, H. and Luo, L. (2002). Representation of the glomerular olfactory map in the Drosophila brain. *Cell* **109**, 243-255.

Python, F. and Stocker, R. F. (2002). Adult-like complexity of the larval antennal lobe of D. melanogaster despite markedly low numbers of odorant receptor neurons. *J. Comp. Neurol.* **445**, 374-387.
Schubiger, M., Tomita, S., Sung, C., Robinow, S. and Truman, J. W. (2003). Isoform specific control of gene activity in vivo by the Drosophila ecdysone receptor. *Mech. Dev.* **120**, 909-918.
Singh, R. N. and Singh, K. (1984). Fine structure of the sensory organs of Drosophila melanogaster Meigen larva (Diptera: Drosophilidae). *Int. J. Insect Morphol. Embryol.* **13**, 255-273.
Stocker, R. F. (1994). The organization of the chemosensory system in *Drosophila melanogaster*: a review. *Cell Tissue Res.* **275**, 3-26.
Stocker, R. F., Heimbeck, G., Gendre, N. and de Belle, J. S. (1997). Neuroblast ablation in Drosophila P[GAL4] lines reveals origins of olfactory interneurons. *J. Neurobiol.* **32**, 443-452.
Technau, G. and Heisenberg, M. (1982). Neural reorganization during metamorphosis of the corpora pedunculata in *Drosophila melanogaster*. *Nature* **295**, 405-407.
Tissot, M. and Stocker, R. F. (2000). Metamorphosis in drosophila and other insects: the fate of neurons throughout the stages. *Prog. Neurobiol.* **62**, 89-111.
Truman, J. W. (1990). Metamorphosis of the central nervous system of *Drosophila*. *J. Neurobiol.* **21**, 1072-1084.
Truman, J. W. and Reiss, S. E. (1976). Dendritic reorganization of an identified motoneuron during metamorphosis of the tobacco hornworm moth. *Science* **192**, 477-479.
Vosshall, L. B., Amrein, H., Morozov, P. S., Rzhetsky, A. and Axel, R. (1999). A spatial map of olfactory receptor expression in the Drosophila antenna. *Cell* **96**, 725-736.
Vosshall, L. B., Wong, A. M. and Axel, R. (2000). An olfactory sensory map in the fly brain. *Cell* **102**, 147-159.
Watts, R. J., Hoopfer, E. D. and Luo, L. (2003). Axon pruning during Drosophila metamorphosis: evidence for local degeneration and requirement of the ubiquitin-proteasome system. *Neuron* **38**, 871-885.
Watts, R. J., Schuldiner, O., Perrino, J., Larsen, C. and Luo, L. (2004). Glia engulf degenerating axons during developmental axon pruning. *Curr. Biol.* **8**, 678-684.
Weeks, J. C. and Truman, J. W. (1985). Independent steroid control of the fates of metamorphosis and their muscles during insect metamorphosis. *J. Neurosci.* **5**, 2290-2300.
Wong, A. M., Wang, J. W. and Axel, R. (2002). Spatial representation of the glomerular map in the *Drosophila* protocerebrum. *Cell* **109**, 229-241.
Yasuyama, K., Meinertzhagen, I. A. and Schurmann, F. W. (2002). Synaptic organization of the mushroom body calyx in Drosophila melanogaster. *J. Comp. Neurol.* **445**, 211-226.
Zheng, X., Wang, J., Haerry, T. E., Wu, A. Y., Martin, J., O'Connor, M. B., Lee, C. H. and Lee, T. (2003). TGF-beta signaling activates steroid hormone receptor expression during neuronal remodeling in the Drosophila brain. *Cell* **112**, 303-315.